RIGA TECHNICAL UNIVERSITY
Faculty of Electronics and Telecommunications
Department of Transport Electronics and Telematics

Vadims BISTROVS
Doctoral student of the programme „ Computer Management, Information and Electronic Systems of Transport”

PERFORMANCE INCREASING OF LOW-COST INTEGRATED GPS/IMU SYSTEM FOR LAND VEHICLE NAVIGATION

Summary of the doctoral thesis

Scientific adviser
Dr.sc.ing., Professor
A. KLUGA

RTU Press
Riga 2014

UDK 629.056.6(043.2)
Bi 902 p

Bistrovs V. Performance increasing of low-cost integrated GPS/IMU system for land vehicle navigation.
Summary of Doctoral Thesis .- R.: RTU Press, 2014.- 39 p.

Published according to the decision of the Promotion Council RTU ETF „RTU P-08” of March 27, 2014, minutes No. 20.

This work has been supported by the European Social Fund within the project «Support for the implementation of doctoral studies at Riga Technical University».

ISBN 978-9934-10-579-1

PROMOTION WORK
SUBMITTED FOR THE DEGREE OF A DOCTOR OF ENGINEERING SCIENCES (TELECOMMUNICATIONS) TO BE DEFENDED AR RIGA TECHNICAL UNIVERSITY

The promotion work for a doctor's degree of engineering sciences (telecommunications) is to be defended publicly on 27 of june at 10:00 o'clock, 2014 at the faculty of Electronics and Telecommunications of Riga Technical University, 16/20 Azenes Str., in the lecture-room 437.

OFFICIAL REVIEWERS

Senior researcher, *Dr. sc. comp.* Modris Greitans
Institute of Electronics and Computer Science, Latvia

Profesor, *Dr. habil. sc. ing.* Igor Kabashkin
Transport and Telecommunication Institute, Latvia

Asoc. Profesor, *Dr. sc. ing.* Victor Boicov
Information Systems Management Institute, Latvia

CONFIRMATION

I confirm that I have developed this promotion work for a doctor's degree of engineering sciences which has been submitted for reviewing at the Riga Technical University. The promotion work is not submitted in any other university for a scientific degree.

Vadims Bistrovs …….(Signature)

Date: ……

The promotion work is written in the English language. It contains Introduction, 8 Chapters, Conclusion, and Bibliography, 219 figures and illustrations, with the total number of 197 pages. The Bibliography has 100 titles.

TABLE OF CONTENTS

List of acronyms and abbreviations

AF	Autocorrelation function
AI	Artificial intelligence
AV	Allan variance
DGPS	Differential GPS
DR	Dead reckoning
EKF	Extended Kalman filter
ENU	East-north-up
GNSS	Global navigation satellite system
GM	Gaussian Markov
GPS	Global positioning system
IKF	Intellectual Kalman filter
IMU	Inertial measurement unit
INS	Inertial navigation system
ISA	Inertial sensor assembly
IS	Inertial sensor
LKF	Linear Kalman filter
LPF	Low pass filtering
LVNS	Land vehicle navigation system
MEMS	Microelectromechanical systems
MSE	Mean square error
RMSE	Root mean square error
PDF	Probability distribution function
PDR	Pedestrian dead reckoning
PF	Particle filter
RADAR	Radio detection and ranging
SINS	Strapdown INS
UKF	Unscented Kalman filter
WD	Wavelet decomposition
ZVU	Zero velocity update

List of mathematical symbols

I_a	Raw acceleration measurement, [m/s^2]
I_g	Raw gyroscope measurement, [deg/s]
a	Acceleration true value, [m/s^2]
ω	Angular rate true value, [deg/s]
ϕ	Roll, [deg]
θ	Pitch, [deg]
b_g	Gyroscope bias,[deg/s]
b_a	Accelerometer bias,[m/s^2]
S	Scale factor
ε	Sensor measurement noise
v	Land vehicle velocity, [m/s]
s	Distance travelled by land vehicle, [m]
β	Fading factor
γ	Threshold in IKF
ψ	Heading, [deg]
N	VRW, [m/s/ h$^{1/2}$] or ARW, [°/h$^{1/2}$]coefficient
K	ARW coefficient, [m/s^2/h$^{1/2}$], [deg/h /h$^{1/2}$]
B	Bias instability coefficient, [m/s^2], [deg/s]
K	KF gain coefficient
H	Measurement matrix
Φ	State transition matrix
Q	System noise covariance matrix
R	Measurement noise covariance matrix
P	System error covariance matrix

INTRODUCTION

Nowadays, the range of applications of low-cost MEMS based inertial sensors increases rapidly due to the recent advances in their reliability and system characteristics. MEMS technology creates a baseline for the next generation of inertial navigation systems. The applications of inertial sensors are from vehicle navigation and guidance, pedestrian dead-reckoning (PDR) through to smartphone game applications.

The era of inertial navigation began when gyros and accelerometers were used as a guidance tool in the German V2 rockets (1942). These navigation systems were gimbaled or floated systems [39]. These systems were very costly and very expensive to maintain. A next step of navigation system development began, when digital computers (with sufficient computational capabilities and memory options) became available. Analytic one (strapdown systems) replaced the mechanical based implementation of the inertial system orientation module [8]. Next development step began with MEMS technology development. Merging electrical and mechanical systems at micro scale, microelectromechanical systems (MEMS) technology has revolutionized inertial sensors [20].

As the use of high performance inertial systems is limited by their high price and the regulation of governments, specifically low-cost MEMS inertial sensors started to be used widely in civil applications [79], [52], and [2].

Actuality of the thesis

A navigation technique is a method for determining position and velocity, either manually or automatically. Different technologies can be used for determining the position of land vehicles. One of them is an inertial navigation. High-cost navigation systems are quite well developed, but it is not economically efficient to use it for land vehicle navigation. The challenge now is in developing and designing navigation systems using MEMS inertial sensors and its output data processing algorithms [2], [42], [52], [75], and [100].

Nowadays the cost, performance, space parameters and power consumption of the inertial sensors are critical for the vehicle manufacturers. Thus, current inertial sensors development is focused on MEMS technology [42], [52], and [100].

However, the performance of MEMS inertial sensors is limited [2], [100]. The main reason of this is a rapid degradation of the navigation solution, when aiding source is not available. This limitation is caused by a high level of the measurement noise [54], therefore, it is necessary to provide regular updates of measurement data for the INS from other sensors (GPS, odometer, speedometer) in order to limit the errors to an acceptable level [36], [91]. Thus, the sensor data fusion methods should be investigated for achieving a better performance of the MEMS-based navigation systems.

GPS signal outage is one of the primary reasons that affects the reliability and continuity of the navigation solution from GPS [91]. The performance of GPS degrades in harsh environments such as urban areas with high-rise buildings and forested areas, because the GPS signals becomes weak or can even be blocked by buildings or dense woods. In addition, GPS signals are not available in tunnels, underground and underwater. The inertial sensors can provide the position, velocity and attitude estimates during GPS signal outages

The combination of an inertial sensors and GPS is well suited for the development of a range of applications as each system compensates for the other's shortcomings [43], [63]. The main function of the satellite-based navigation system is providing position information, while the main function of the inertial sensors is providing the attitude information of the object. The GPS system can be used for the calibration of inertial sensors, but the inertial sensors can be used for bridging the GPS signal outages [52].

Aims and tasks of the research

The goal of the doctoral thesis is investigating the increasing performance of the low-cost MEMS IMU Motion Node for land vehicle navigation. In order to realize this goal the following tasks were planned:

1. To investigate measurement noise characteristics of MEMS inertial sensors;
2. To develop error signal models of MotionNode IMU accelerometers and gyroscopes;
3. To investigate sensors (GPS, magnetometer, MEMS gyroscope and accelerometer) data processing algorithms;
4. To investigate Kalman-based state estimation algorithms of the low-cost navigation system;
5. To evaluate the performance of the developed navigation system via field tests that include also simulated GPS signal outages.

Scientific novelty and main results

1. The MotionNode MEMS IMU achieves tactical grade IMU performance, using developed sensors data processing algorithms (including sensors data fusion algorithms) for land vehicle navigation system.
2. It was shown that it is necessary to implement systematic sensor calibration and use of special algorithms (the intellectual KF, the adaptive KF) for the sensors data fusion in order to limit the increase in sensors measurement errors.
3. The particle filter estimates the system states with any probability density function. It is an advantage of MEMS inertial sensors data processing. However, for the modern low-cost navigation system, this algorithm is not efficient because of its heavy computational requirements and rather poor stability characteristics.
4. The possibility of using Allan variance and data frame statistical analysis was shown for experimental inertial data processing in order to identify MEMS IMU noise signal models that are used in data fusion algorithms. This allows to increase the performance of GPS/MEMS IMU integrated navigation systems, including maintenance of stand-alone inertial navigation solution during 60-90 s of GPS signal outage that is near to tactical grade IMU performance.
5. The MATLAB scripts were developed. The main scripts are: sensors data preprocessing algorithms, inertial sensors signal analysis using Allan variance algorithm, the LKF algorithm and it improvements, object attitude estimation algorithm (including magnetometer calibration procedure), the EKF, PF, UKF algorithms.

Statements presented for defence

1. It is possible to improve the performance of MEMS IMU up to the level of the tactical IMU including maintenance of given estimation precision for the vehicle velocity and driving distance during 60-90 s GPS outages.
2. Combined GPS/MEMS IMU/magnetometer data processing increases attitude estimation precision up to $\sigma < 0.03^{\circ}$ (zero velocity update) and driving distance estimation precision at least by 30%.
3. The UKF-based low-cost sensors data fusion algorithm improves the GPS/MEMS IMU/magnetometer integrated navigation system performance using the results of the Allan variance and data frame statistical analysis of the inertial sensors signals.
4. It is necessary to define appropriate models of inertial sensors signals and its characteristics for elaboration of the low-cost MEMS-based integrated navigation system with

improved performance. This is the first necessary condition for the elaboration of a low-cost navigation system with improved performance.

5. It was shown that the LKF and the UKF algorithms have similar performance, when land vehicle acceleration is near to zero and GPS signal is not available. In fact when the land vehicle dynamics changes quickly (GPS signal is not available), then the UKF algorithm has better estimation precision of the navigation system state (sensor bias, velocity). The choice of the appropriate system state estimation algorithm is the second necessary condition for the elaboration of a low-cost navigation system with improved performance.

Research methodology

Time series analysis, random process theory, elements and methods of system theory and optimal system state estimation theory were used in this research. The main theoretical methods of the research are summarised in Table 1.

Table 1.

Some examples of the theoretical methods used in research

Theory	Methods
Time series analysis	Frame statistics The AV analysis
Random process theory	State models for the stochastic processes
System theory	State-space representation of the navigation system
Optimal system state estimation theory	The unscented Kalman filter The particle filter

The process of elaboration of algorithms was as follows:

a) scientific publications were analysed in order to find appropriate implementation solutions of navigation systems (including data processing algorithms);

b) field tests were conducted (with land vehicle, where low-cost sensors were installed) in order to obtain data for analysis;

c) MATLAB scripts were developed for data processing;

d) improvements of algorithms were developed and new solutions were proposed taking in account the goal of the work;

e) proposed algorithms were validated via field tests data for different land vehicle movement modes.

Work practical application

1. Recommendations are given for low-cost navigation system elaboration.

2. The possibility of automotive grade IMU use for land vehicle navigation was shown.

3. The MATLAB scripts were created for the inertial system analysis and sensors data fusion.

4. Work scientific results were used in the following scientific projects:

„Objekta telpiskā stāvokļa novērtēsana", project „Inovatīvas signālapstrādes tehnoloģijas viedu un efektīvu elektronisko sistēmu radīšanai" (Valsts pētījumu programma V7692);

„Mobīlo sensoru tīklu struktūras analīze", LZP grant Z09.1552 „Jaunu ciparu signālu apstrādes, mobilo telekomunikāciju tīklu un to elektronisko komponenšu izpētes metožu izstrāde, efektivitātes pētīšana un realizācija".

Approbation of the research results
List of the publications

1. Bistrovs V. Analyze of MEMS Based Inertial sensors Parameters for land Vehicle Navigation Application// *RTU zinātniskie* raksti. 7. sēr., Telekomunikācijas un elektronika. – Riga: RTU, 2008. - Vol. 8. - pp. 43-47
2. Bistrovs V. Analyse of Kalman Algorithm for Different Movement Modes of Land Mobile Object // *Electronics and Electrical Engineering*. – Kaunas: Technologija, 2008. - Nr.6 (86). - pp. 89-92
3. Bistrovs V., Kluga A. Combined Information Processing from GPS and IMU using Kalman Filtering Algorithm // *Electronics and Electrical Engineering*. – Kaunas: Technologija , 2009.- No. 5(93). – pp. 15-20.
4. Bistrovs V., Kluga A. Distance Estimation using Intelligent Fusion of Navigation Data// *Electronics and Electrical Engineering*. – Kaunas: Technologija, 2010.- No. 5(101). - pp. 47-52.
5. Bistrovs V., Kluga A. MEMS INS/GPS data fusion using particle filter// Electronics and Electrical Engineering. – Kaunas: Technologija , 2011. – No. 6(112). – pp. 77–80.
6. Bistrov V. Study of the characteristics of Random Errors in Measurements by MEMS Inertial Sensors// *Automatic Control and Computer Sciences*. - New York : Allerton Press, 2011. - Vol. 45(5).- pp. 284–292.
7. Bistrovs V., Kluga A. Adaptive Extended Kalman Filter for Aided Inertial Navigation System// *Electronics and Electrical Engineering*. – Kaunas: Technologija, 2012. – No. 6(122). – pp. 37–40.
8. Bistrov V. Performance analysis of alignment process of MEMS IMU // International Journal of Navigation and Observation. - Hindawi Publishing Corporation, 2012.- Volume 2012.
9. Bistrovs V., Kluga A. The Analysis of UKF based Navigation during GPS outage// *Electronics and Electrical Engineering*, – Kaunas: Technologija, 2013. – Vol. 19, No 10. – pp. 13 – 16.

Participation in the international conferences

1. *12TH INTERNATIONAL CONFERENCE of ELECTRONICS, Lithuania, Kaunas, May 05, 2008*
Analyse of Kalman algorithm for different movement modes of land mobile object.

2. *Riga Technical University 49th International Scientific Conference,* Latvia, Riga, October 11-13,2008 MEMS IMU parameter analysis for land vehicle navigation application

3. *13TH INTERNATIONAL CONFERENCE of ELECTRONICS, Lithuania, Vilnius, May 14,2009,*
Combined Information processing from GPS and IMU using Kalman filtering algorithm.

4. 14TH INTERNATIONAL CONFERENCE of ELECTRONICS, Lithuania, Kaunas, May 18, 2010
Distance Estimation using Intelligent Fusion of Navigation Data.

5. *Riga Technical University 52nd International Scientific Conference,* Latvia, Riga, October 13-14,2011 Performance Analyse for MEMS IMU Alignment Process

6. 15TH INTERNATIONAL CONFERENCE of ELECTRONICS, Vilnius, May 19, 2011
MEMS INS/GPS data fusion using particle filter

7. 16TH INTERNATIONAL CONFERENCE of ELECTRONICS, Palanga, June 18-20, 2012

Adaptive Extended Kalman Filter for Aided Inertial Navigation System

8. 17TH INTERNATIONAL CONFERENCE of ELECTRONICS, Palanga, June 17-19, 2013
The Analysis of the UKF-Based Navigation Algorithm during GPS Outage

Participation in international conferences not related with the subject of the promotion work

1. *12TH INTERNATIONAL CONFERENCE of ELECTRONICS, Lithuania, Kaunas,* 21.05.2008
Response time and probability of packet loss in communication system with batch arrivals,

2. *12TH INTERNATIONAL CONFERENCE of ELECTRONICS, Lithuania, Kaunas,* 21.05.2008
Comparing batch and self-similar arrivals in communication systems,

Structure of the thesis

Doctoral thesis consists of eight chapters, conclusion and list of references. The thesis contains 197 pages, 219 figures, 37 tables and a reference list of 100 sources. The description of the GNSS and inertial navigation system, the sensors data fusion possibilities, MEMS-based inertial sensors characteristics are given in the 1st and 2nd chapter. The analysis of the measurement error signal of the MEMS inertial sensors can be found in the 3rd chapter. Here, the sensor measurement error models are elaborated. The 4th chapter gives explanation about coordinate frames that used in the inertial navigation and investigates impact of the correction for inertial data due to the coordinate frame transformation. The problems of the alignment of the low-cost inertial navigation system and attitude estimation are discussed in the 5th chapter. Theoretical background of the data fusion algorithm and practical implementation and experimental results of the sensors data processing for the estimation of navigation parameters are considered in the 6th and 7th chapter. Finally, the performance of the estimation algorithm during GPS outage is analyzed in the 8th chapter. Then, conclusions and summary of the main results are given. The main conclusions, list of tests, and created programs using MATLAB® are reported in the end of chapters.

1. NAVIGATION SYSTEMS

Navigation system is a system, which aids in navigation. The different types of the navigation systems exist in the world. The inertial navigation and radio navigation systems (e.g. GNSS) are the most popular navigation system.

1.1. GNSS

The most popular satellite navigation system is GPS. GPS consists of three segments: the space segment (consist of satellites), the control segment (infrastructure for maintain and control of the navigation system), and the user segment (e.g. GPS signal receivers). Satellites continuously transmit radio signal (two spread spectrum with carrier frequency 1575.42 MHz and 1227.6 MHz) and user equipment receives it. It is necessary to have signal from four satellites in order to define position of the user (4th satellite is necessary for calculating receiver time offset, as theoretically only three satellites are necessary for user position determination) [17].

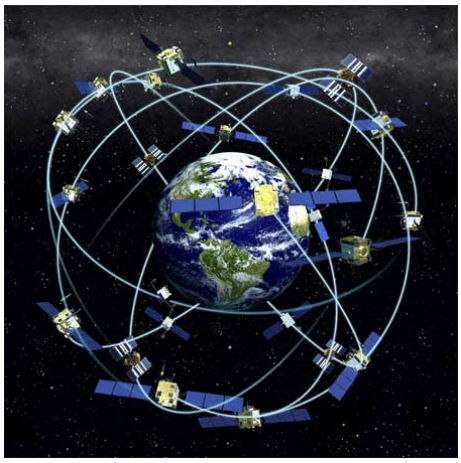

Fig. 1.1. 24-satellite constellation of GPS space segment [30]

The GPS measurements, like all measurable quantities, contain errors and biases, which can be removed or reduced by combining the various GPS observables. In principle, there are three groups of the GPS errors and biases: satellite-related, receiver-related, and atmospheric errors and biases.

Even under the full constellation of 24 GPS satellites, some periods of time exist when four satellites are not visible above a particular elevation angle. Such a satellite visibility problem is expected more at high latitudes (higher than about 55°), because of the nature of the GPS constellation (Fig. 1.1). This problem may also occur in some low- or midlatitude areas for a particular period of time. In urban and forested areas, the receivers sky window is also reduced as a result of the obstruction caused by the high-rise buildings and the trees [2], [13], [16], [17], [20].

1.2. Inertial navigation system

The core units of inertial systems are accelerometers and gyroscopes. An accelerometer measures the specific force in an inertial reference frame. Then this measurement is used for acceleration estimation of the moving object (land vehicle, person, etc). The gyroscope is used for angular rate measurement with respect to the inertial frame. The inertial sensors do not require external signal for operating. This means that measurements of inertial sensors are available at all conditions and in all environments.

Basically, inertial navigation system (INS) consists of inertial measurement unit (IMU), inertial sensor data processing unit (navigation processor), power supply and user interface. IMU consists of the accelerometers and gyroscopes (inertial sensor assembly) and additional electronics for sensor control and sensor signal processing.

The IMU can be classified taking in account it precision and the level of noises. The most commonly used classes or grades of the IMU are strategic, navigation (aviation), tactical and automotive [17]. The automotive grade IMUs are considered in this work.

The strong points of inertial navigation systems are:

a) it is self-contained system that does not need any external signals;

b) the integration of the accelerometer and gyroscope outputs can already give useful navigation measures such as change of velocity and attitude of the vehicle;

c) low level of short term noise;

d) high bandwidth of the signal.

The INS can be gimballed or strapdown [16]. Strapdown inertial system is considered in this work.

1.3. Aided navigation system

Several possibilities exist for MEMS inertial sensors aiding. The classification of the aiding sources can be following [2]:

a) aiding in coordinate domain (GNSS, RADAR etc);

b) aiding in velocity domain (zero velocity updates, nonholomic constraints, odometer);

c) aiding in attitude domain (MEMS magnetometers, map matching).

The combined processing of sensors data should be realized, when several sensors are used in the navigation system. This, in turn, allows realizing more robust, informative, reliable and precise navigation system.

Depending on application of the navigation system, it's necessary to define types of the sensors, which will be involved in estimation of the navigation solution. Heading and longitudinal acceleration of the vehicle is one of the important estimated parameters for land navigation. Hence, longitudinal accelerometer, vertical channel gyro (or horizontal plane magnetometers) and GPS as aiding source are enough for land vehicle navigation.

1.4. GPS/IMU integration schemes

Roughly, two main GNSS/INS integration schemes are used in the design of integrated navigation system. These schemes are tightly and loosely coupled GPS/INS integration schemes.

In loosely coupled integration scheme the GPS-derived position and velocity is used for correcting inertial navigation solution. This integration scheme is based on the independence of the GPS and inertial navigation functions.

In tightly coupled schemes the pseudo-range or pseudo-rate measurements are used as aiding information. The main advantage of this technique is maintaining of inertial system aiding even if signal from one satellite is available. The main disadvantage of this scheme is lack of the standalone GPS solution [17]. However, tightly coupled algorithms require more computational resources comparing with loosely coupled schemes. In addition, the measurement model is more complex in integration schemes. The larger dimension of the state vector in tightly coupled integration scheme increases the time for filter convergence [16]. Therefore, the loosely coupled integration scheme becomes popular for implementing in many applications.

1.5. Estimation algorithms of the navigation system

Different types of the estimation algorithms can be used in the navigation systems. The main types of those algorithms are Kalman filter (KF) based algorithms (including standard KF, extended KF, and unscented KF), artificial intelligence (AI) based methods (artificial neural networks and adaptive fuzzy systems) [2], [17]. The main difference between KF-based and AI-based algorithm is that AI-based methods do not use any predefined mathematical description of the system and measurement model and do not use any statistical information as input [2]. AI methods require empirical learning that takes considerable time and resources. The only case, when AI-based methods can provide superior performance is during long outages of the measurement updates (e.g. during GPS signal outages). The KF requires definition of the appropriate model of the system dynamics. If the processed data by the KF does not fit the model, estimation of the navigation parameters will be not optimal. The estimation of the states of the low-cost land vehicle navigation system is considered as nonlinear problem. Hence, the estimation algorithm should be capable dealing with nonlinear dynamic system. The EKF is one of the widely used algorithms for such a navigation systems

[17], [25] . In practice, however, the EKF has several limitations. First, the derivation of the Jakobian matrices for both the system and measurement equations can be nontrivial and lead to significant implementation difficulties. Second, only small errors states should be processed by the EKF, otherwise the first order approximations can cause biased solution and even can lead to filter instability [14]. In order to avoid this problems and enhance estimation results of the nonlinear systems, it is recommended to use the UKF algorithm [17], [24], [27]. The key idea of the UKF is that it would be easier to approximate a Gaussian distribution than to approximate an arbitrary nonlinear function or transformation. The UKF has a big potential for application in low-cost land navigation system, because of its convenient and straightforward method of the system and measurement model definition comparing with the EKF. In addition, the UKF provides more efficient tuning possibilities for adjusting filter for optimal work. The main problem, when implementing the UKF algorithm, was avoiding covariance matrix to be non positive definite.

The particle filters are usually not implemented for high dimension of the system [18].

2. MEMS-BASED INERTIAL SENSORS

The first micro machined accelerometer was designed in 1979 at Stanford University, but it took over 15 years before such devices became accepted mainstream products for large volume applications. Micro-fabrication is the set of technologies used to manufacture structures with micrometric features (e.g. MEMS sensors). MEMS technologies are offering low-cost, small size (below 100 micrometers), and light weight (< 1g) sensors with low power consumption [1], [16].

In comparison to the accelerometers, gyroscopes are a challenging technology that is in the development stage. MEMS gyroscopes use Coriolis effect to sense rotation [1].

2.1. Real world MEMS based IMUs

The MTi-G device from Xsens motion technologies and MotionNode IMU from GLI Interactive LLC were used as low-cost IMUs for the research.

The MTi-G device is an integrated GPS and MEMS Inertial Measurement Unit with a navigation and attitude and heading reference system processor. The internal low-power signal processor runs a real-time Xsens Kalman Filter (XKF) providing inertial enhanced 3D position , velocity and attitude estimates.

The MotionNode IMU is a 3-DOF inertial measurement unit.

2.2. Model of the inertial sensor signal

There are two types of MEMS IS measurement errors: systematic (run-to-run bias, scale factor, sensor axis misalignment error) and random (scale factor and in-run bias fluctuations, noise).

A number of inertial sensor calibration methods exist for systematic part of measurement error reduce. A detailed description of these methods can be found in [2].

Random errors can be approximated using stochastic process models.

The systematic errors can be determined and compensated for during calibration by the manufacturer; therefore, the measurements of the sensors of the considered IMU can be represented as follows:

$$I_a = a + b_{a,rand} + S_{a,rand} \cdot a + \varepsilon(a), \tag{2.1}$$

$$I_g = \omega + b_{g,rand} + S_{g,rand} \cdot \omega + \varepsilon(\omega), \tag{2.2}$$

The random bias of the MEMS IS in expressions (2.1) and (2.2) can be separated into two parts [17]:

$$b_{a,rand} = b_{as} + b_{ad},$$
$$b_{g,rand} = b_{gs} + b_{gd}, \quad (2.3)$$

where b_{as} and b_{gs} are the static and b_{ad} and b_{gd} are the dynamical parts of the bias.

The static part of random bias is a fixed bias involving the run-to-run changing bias, as well as an uncompensated bias, in the course of the calibration by the manufacturer. This part of the bias remains constant during the inertial sensor (IS) operating within a single run. The dynamic part of the bias, which is known as the drift of the bias, varies with a time period of one minute (depending on the ISs characteristics) and includes a residual (uncompensated during the calibration) bias depending on the ambient temperature. The dynamic part of random bias is modelled as random process [2].

Similarly, the scaling factor can be separated into static and dynamic components.

2.3. Calibration of the inertial sensors

In order to estimate uncompensated bias (systematic and random static) and scale factor of the accelerometers of IMU Motion Node, the six point calibration procedure can be performed in stationary mode [17]. The calculated bias and scale factor are shown in the Table 2.1. The bias estimation results show that IMU MotionNode belongs to consumer/automotive grade device.

Table 2.1.

Bias and scale factor of MotionNode IMU accelerometers [4]

	X-axis	
	bias,m/s^2	**SF**
mean	-0.1418	-0.0043
deviation	0.0014	9.6177e-005
	Y-axis	
mean	0.2275	-0.00079
deviation	0.0023	4.9800e-004
	Z-axis	
mean	-0.1060	-0.0019
deviation	0.0020	1.6733e-004

If it is assumed that maximal acceleration, experienced by land vehicle is 3 m/s^2, then it is possible to neglect impact of the scale factor error on total error contribution of the accelerometer signal. Finally, the model of the accelerometer signal can be expressed as

$$I_a = a + b_{a,rand} + \varepsilon(a), \quad (2.4)$$

2.4. Land vehicle dead reckoning system

Now the performance of the dead reckoning system with one longitudinal accelerometer will be checked. The accelerometer signal model (2.4) is used. During experiments Motion

Node IMU was rigidly fixed and leveled inside vehicle. The direction of the vehicle movement and accelerometer sensitive axis coincide. The route taken during experiments is shown in Fig. 2.1.

Fig. 2.1. Route taken for experiments [6]

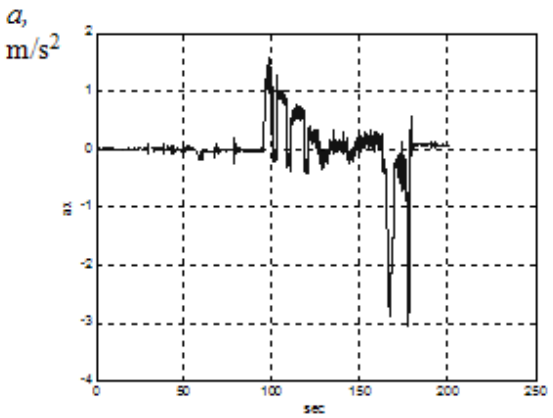

Fig. 2.2. Accelerometer (x-axis) calibrated signals

The accelerometer data was recorded on HDD and then processed for obtaining estimation of the vehicle velocity and traveled distance according following steps:

1. Calculation of the accelerometer bias via averaging of the accelerometer static signal;
2. Calculation of the vehicle velocity and traveled distance via integration of true acceleration.

The calculation results, when vehicle velocity during it uniform moving was around 60 km/h and traveled distance was 1020 m, are shown in Fig. 2.3-2.4. These rather good estimations of the velocity and driving distance were due to the implemented rule-based artificial algorithm for the acceleration signal processing. According this rule stationary accelerometer measurements are replaced by zero, when the acceleration value is less than estimated standard deviation of the static accelerometer signal.

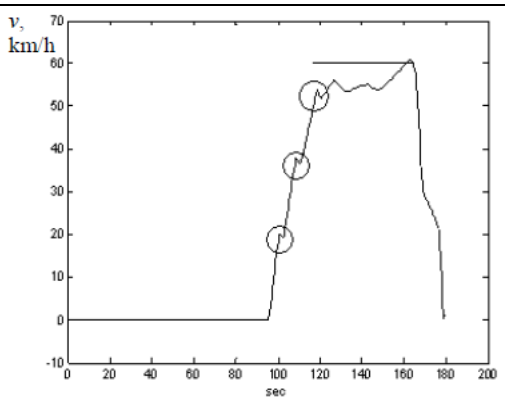

Fig. 2.3. The velocity of vehicle estimation

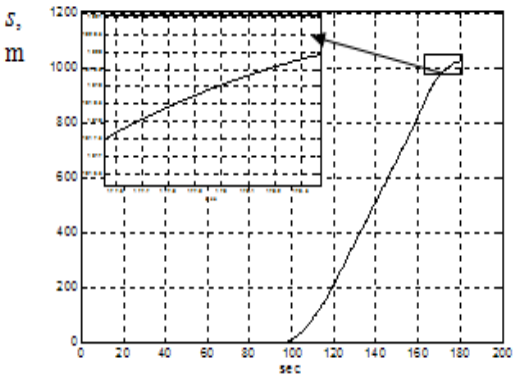

Fig. 2.4. The driving distance estimation (s = 1020 m)

This simple example showed

1. The velocity and distance can be easily calculated without noisy fluctuations via integration of the accelerometer signal (here, integration has a function of the LP filter);
2. The IMU is self-contained unit without necessary to have external signal for operating;

3. It is not shown here, but it is evident that the estimation error of position and velocity increases rapidly with time if the accelerometer bias is not removed before integration of the acceleration;

4. The IMU should be properly aligned and fixed inside vehicle for increasing position and velocity estimation accuracy;

5. The estimated values have perfect short term accuracy (see Fig. 2.3, where moments of vehicle gear shifting are identified).

In the considered above examples, it was assumed that accelerometer measurement error consists of constant in-run bias and gaussian noise. In fact the in-run bias is not constant for MEMS accelerometers and noises can have quite complicated nature and combination. MEMS gyroscopes have even more complex nature of the measurement error due to lack of the design maturity. In order to reduce negative impact of this measurement errors, quite sophisticated methods and algorithms should be developed, such as sensor data fusion algorithms.

2.5. High frequency noise reduction

The integration with GPS reduces only long term errors of the inertial system. In order to reduce high frequency noise , sensors signal processing methods, such as low-pass filtering, wavelet decomposition or LKF, should be implemented. LKF provides not only high frequency error decreasing, but also removes accelerometer bias (Fig. 2.5), which was included in the system model of the LKF.

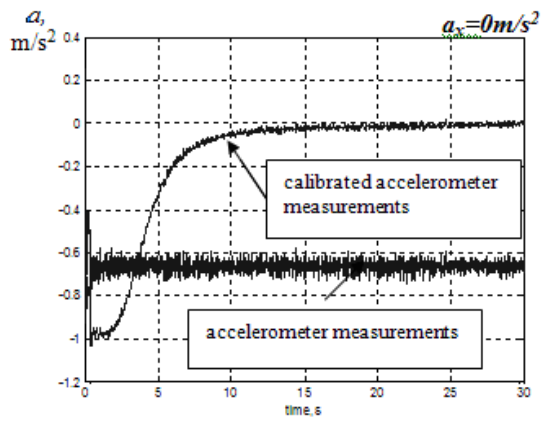

Fig. 2.5. Accelerometer measurements before and after post calibration process.

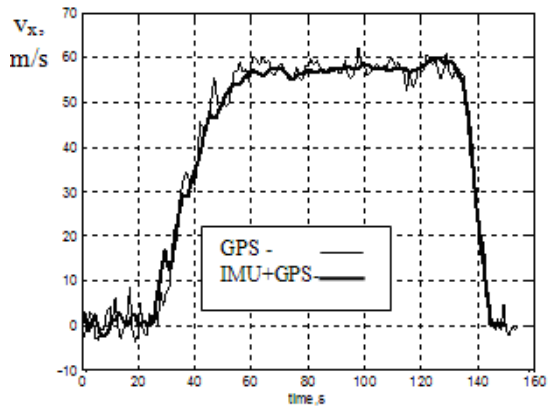

Fig. 2.6. Estimation of vehicle velocity, when v = 60 km/h.

In turn, accelerometer aiding helps to reduce high frequency errors of the GPS derived velocity estimate. As an example, there are quite big noisy fluctuations of the velocity estimation based on GPS measurements (see Fig. 2.6). The fluctuations of estimated velocity decrease if the combined processing of the accelerometer and GPS data is done using the LKF [6].

3. MEMS-BASED INERTIAL SENSORS SIGNAL ANALYSIS

The analysis of the signals in the time and frequency domain was made in order to investigate characteristics of the measurement errors of MEMS inertial sensors. Signal of the static accelerometer is shown in Fig. 3.1

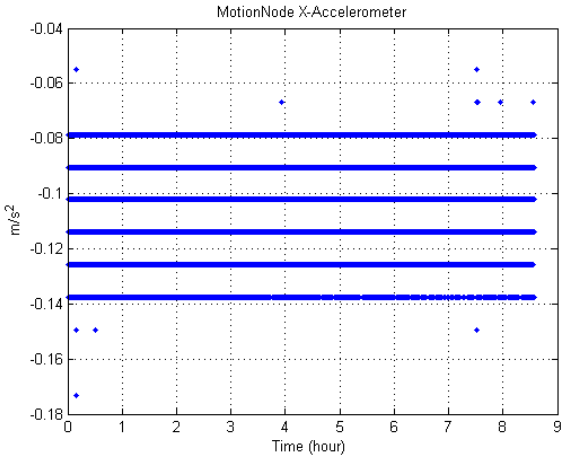

Fig. 3.1. Static data (8 hours) of x-accelerometer of the MotionNode IMU

Each point in Fig. 3.1 corresponds to the single measured value. As the measurement rate of accelerometer was 60 Hz and measurement was conducted during 8 hours, the points create corresponding lines. From Fig. 3.1, the resolution of accelerometer signal can be easily defined.

The mode value of the static accelerometer signal can be used as estimation of constant bias term.

3.1. Variations of the inertial sensors signals due to the temperature

It is necessary to take in account variation of the sensors signal due to the temperature change for the IMU without efficient algorithm of the temperature compensation. The variation of the output signal during IMU heating is shown in Fig. 3.2 and 3.3. The time necessary to stabilize the mean value of accelerometer bias can be up to 20 min for Motion Node IMU.

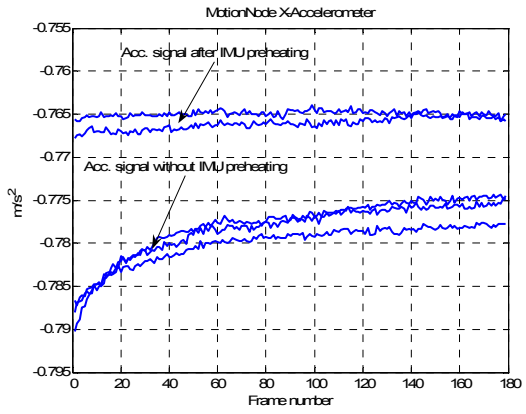

Fig. 3.2. Estimates of mean value of static accelerometer signal (1 hour) versus frame number (frame length=1000 measurements)

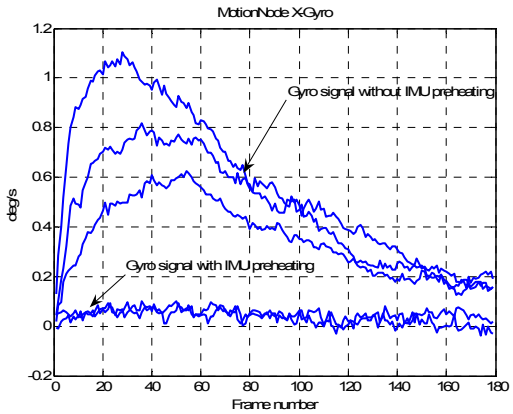

Fig. 3.3. Estimates of mean value of static gyroscope signal (1 hour) versus frame number (frame length= 1000 measurements)

3.2. Accelerometer measurement error reduction

The combined use of the LPF and the LKF allows considerably reduce sensor measurement error (Fig. 3.4).

This combination gives reduction of noise at least two times more comparing with use of LKF alone.

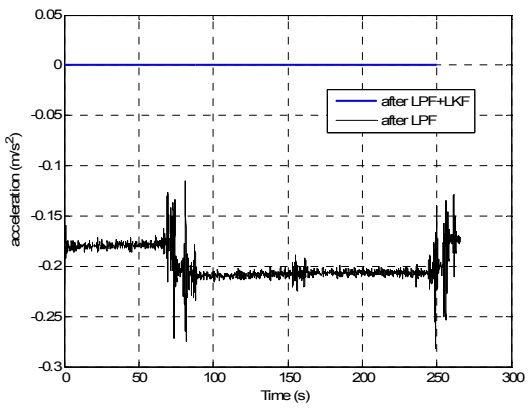

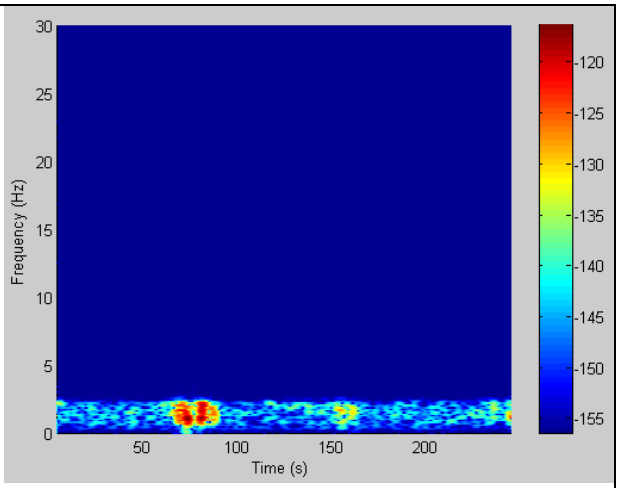

Fig. 3.4. Longitudinal acceleration signal analysis (TEST Jan7). Signal denoising using LPF+ LKF. The SD of the denoised signal is $\sigma = 3.34 \cdot 10^{-7}$ m/s^2. 9th order Chebyshev type II digital filter (stopband edge frequency equals 3 Hz, stopband ripple equals 60 dB down)

When reducing high frequency errors, it is necessary to remember about maintaining of true motion spectrum in signal.

3.3. Identification of the measurement error type of the inertial sensors

First, the types of the random sensor measurement errors should be identified. Then, the random errors are described using stochastic process models. Then, these models will be included in the estimation algorithm of the navigation system. The inertial sensor random errors can be described using following stochastic models or its combination: white noise, random constant, random walk, first-order Gauss-Markov model (GM). For most of the low-cost inertial sensors 1st order Gauss-Markov or random walk and white noise models can be used for stochastic error description [17].

The noises of the dynamic component of the sensor bias are identified using Allan variance method, a detailed description of which can be found in the standard IEEE STD 647-2006. In order to calculate the Allan variance function, the signal is divided into different numbers of segments characterized by the same averaging time τ. The Allan variance for each individual time interval is determined from the formula

$$\sigma^2(\tau) = \frac{1}{2 \cdot (N-1)} \sum_{i=1}^{N-1} \left(\overline{s_{i+1}}(\tau) - \overline{s_i}(\tau) \right)^2, \tag{3.1}$$

The calculated noise parameters for the IS of IMU MotionNode are given in Tables 3.1 and 3.2 [8].

As expected, the maximum instability and large noises are exhibited by sensors of the y-axis (the vertical channel of the MotionNode IMU) due to the influence of the Earth's gravity. The AV analysis shows that the sources of errors in the accelerometer signal are the noises of the velocity random walk and acceleration random walk. For the y-accelerometer, there is also a correlated noise (τ = 3.8 s). For the gyroscope, the noises of the angle random walk and rate random walk, as well as the flicker noise (corresponding to the range of instability of the zero bias on the function of Allan variance), are dominant; the latter is slightly more expressed than for the accelerometers, where there is almost no flicker noise.

Table 3.1.

Noise parameters for accelerometers of IMU MotionNode

	N, m/s/ $h^{1/2}$	AC	ε,%	K, $m/s^2/h^{1/2}$	AC	ε,%	B, m/s^2	ε,%
X	0.06	-0.48	±2.4	$9.326 \cdot 10^{-4}$	0.50	±15	$2.233 \cdot 10^{-4}$	±3.4
Y	0.057	-0.49	±2.2	0.0051	0.65	±15	$3.602 \cdot 10^{-4}$	±2.1
Z	0.06	-0.46	±2.1	0.0021	0.57	±15	$2.8833 \cdot 10^{-4}$	±2.6

Table 3.2.

Noise parameters for gyroscopes of IMU MotionNode

	N, deg/$h^{1/2}$	AC	ε,%	K, deg/h /$h^{1/2}$	AC	ε,%	B, deg/h	ε,%
X	1.94	-0.38	±1	275	0.51	±15	54	±5.6
Y	2.71	-0.36	±0.6	2969	0.63	±15	143	±1.7
Z	2.16	-0.40	±0.6	-	-		75	±7.9

It can be seen from the plots (Fig. 3.5) that the curves of Allan variance vary from one run to another. The greatest difference is observed in the range of averaging times $\tau > 30$ s for accelerometers and $\tau > 100$ s for gyroscopes [8].

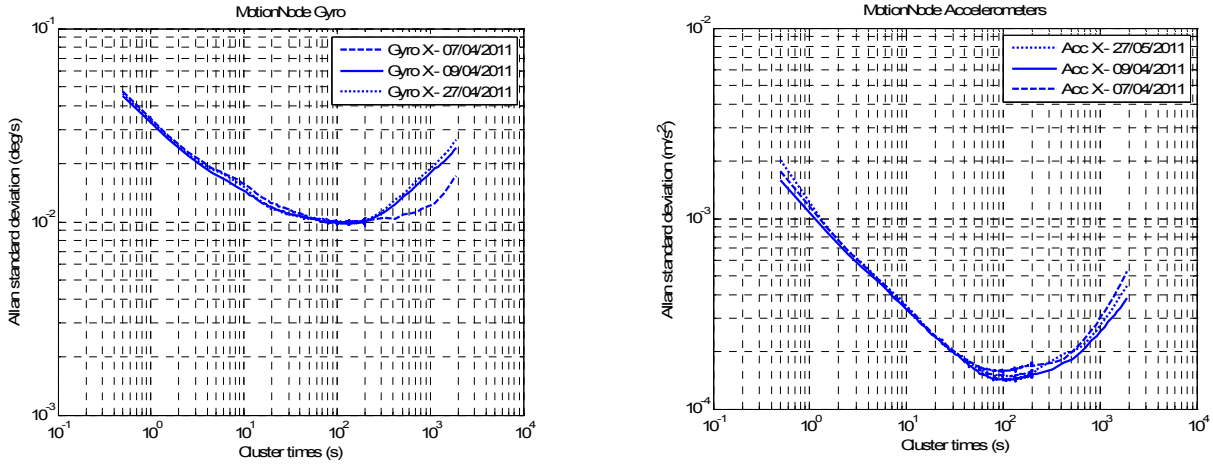

Fig. 3.5. Curves of Allan's variance of the MotionNode IMU IS from one run to another

The elaborated models for in-run bias of the IS of MotionNode IMU are given in Table 3.3.

Table 3.3.

Error models of in-run bias for IMU MotionNode inertial sensors

Model validity period	Till several seconds	Till few minutes
X-accelerometer	white noise	SF+Δ, $\Delta_{max} \approx 10^{-3}$
Z-accelerometer	white noise	SF+Δ, $\Delta_{max} \approx 10^{-3}$
Y-gyroscope	sum of GM and DF(2)	sum of GM and DF(2)

The stochastic function (SF) can be defined by GM process or sum of GM and white process. The deterministic function (DF(n))is defined by polynomial of n degree.

4. ALIGNMENT OF THE IMU AND ATTITUDE ESTIMATION

The IMU axes should be aligned with vehicle axes (to make the b-frame that coincide with the v-frame), before estimation of the navigation parameters. Then, the body frame is aligned with navigation frame. During the process of absolute alignment the pitch, roll and heading angles are estimated.

The requirements of the initial alignment of the IMU are high accuracy and short time. An accurate alignment is very important for precise estimation of the navigation parameters. But accurate alignment can take considerable amount of time. Thus a compromise of accuracy and time consumption of the initial alignment should be made.

However, MEMS sensors have significantly high drift rates and noise characteristics, and, therefore, the gyroscope outputs cannot be used to estimate the azimuth or heading of the vehicle.When the GPS signal is available and the vehicle has a non-zero velocity, it is possible to calculate a heading of the vehicle using the GPS-derived velocity. When the GPS signal is not available, the magnetometers (which sense the Earth's geomagnetic field strength) can be used for determination of the absolute heading with reference to the local magnetic North.

The quaternion based KF was proposed for estimation of the object attitude. To test the proposed attitude calculation method, the attitude result is compared with the attitude output of the IMU MTi-G. The attitude output from the IMU MTi-G and the proposed method with the calibrated data from the IMU MTi-G uses the same data, thus the attitude result comparison means only the comparison of the differences in the attitude calculation by the algorithms. The GPS signal for the IMU MTi-G was unavailable during the tests. Experiments for attitude estimation were conducted through simulating the certain value of pitch and roll angles of the IMU MTi-G using a tilt table. The results of the attitude estimation are given in Table 4.1-4.3 [10].

Table 4.1.

The statistical characteristics of the estimated pitch and roll ($\theta = 0°$ and $\phi = 0°$ with a precision ±0.1°)

Statistical characteristics, degree, [°]	Pitch estimation by		Roll estimation by	
	MTi-G	Proposed algorithm	MTi-G	Proposed algorithm
Mean value	-0.4699	-0.3142	0.3433	0.4896
Standard deviation	0.1270	0.0168	0.1949	0.0150

Table 4.2.

The statistical characteristics of the estimated pitch and roll ($\phi = 39.5°$ with a precision ±0.5°, and $\theta = 0°$)

Statistical characteristics, degree, [°]	Pitch estimation by		Roll estimation by	
	MTi-G	Proposed algorithm	MTi-G	Proposed algorithm
Mean value	39.7758	39.4934	39.3042	39.6591
Standard deviation	0.1336	0.0307	0.3483	0.0318

Table 4.3.

The statistical characteristics of the estimated heading

Statistical characteristics, degree, [°]	Heading estimation by	
	MTi-G	Proposed algorithm
Mean value	119.0114	118.5133
Standard deviation	0.8005	0.4083

MEMS IMU is capable to estimate the initial attitude angles (the pitch and roll) in the stationary mode without correction from an external sensor such as the GPS. The attitude estimation precision (±0.5°) is sufficient for a vehicle navigation application. The convergence rate of the proposed algorithm is very fast: less than 1 second is necessary to obtain the estimations of the pitch and roll.

It is possible to decrease the standard deviation of the pitch/roll estimation for a stationary object even more. For this purpose, the state transition matrix **Φ** in the KF algorithm should be replaced by the corresponding identity matrix (**Φ = I**). The system noise level should be decreased for at least 1000-10000 times comparing to the value defined according to the MEMS gyroscope specification. The results of the attitude estimation (when pitch and roll are zero) after such modification are given in Table 4.4 [10].

Table 4.4.

The statistical characteristics of the estimated pitch and roll (**R**=0.01·**I**)

Statistical characteristics, degree, [°]	Pitch estimation by		Roll estimation by	
	KF	Modified KF	KF	Modified KF
Mean value	0.2648	0.2646	0.4512	0.4510
Standard deviation	0.0096	0.0040	0.0128	0.0055

The impact of the system noise value σ in the LKF for the standard deviation of the roll and pitch estimation was analysed (Fig. 4.1, 4.2).

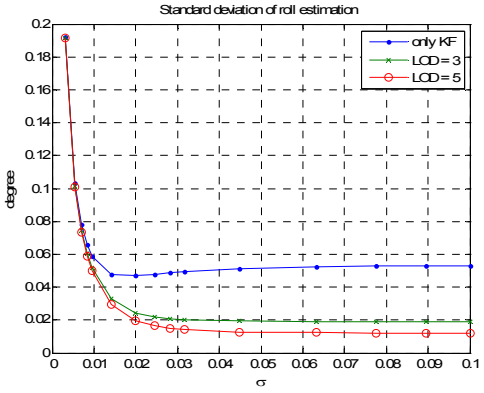

Fig. 4.1. Impact of the system noise value σ for the standard deviation of the roll estimation (LOD - Level of Decomposition)

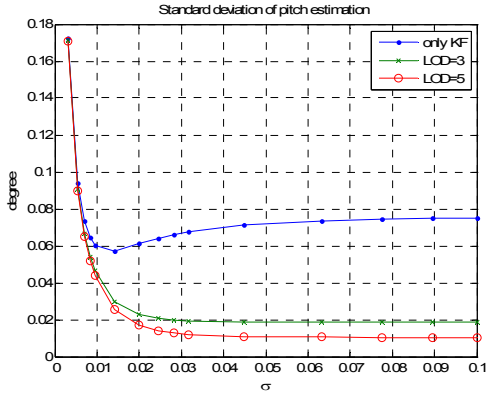

Fig. 4.2. Impact of the system noise value σ for the standard deviation of the pitch estimation (LOD-Level of Decomposition)

The standard deviation of the pitch/roll estimation has greater minimal value, when the LKF algorithm is used without signal preprocessing by a wavelet algorithm. And there is only one optimal value of the system noise deviation σ that minimizes the standard deviation of the pitch/roll estimation, when only LKF algorithm is used for data processing.

In most cases, it is sufficient to have accelerometer data for pitch and roll estimation, when a vehicle is in stationary mode. When the vehicle is moving, it is not possible to obtain a reliable solution for the vehicle pitch and roll attitude angles using only accelerometer signals. It is related to the fact that the accelerometer signal contains the information not only about the object misalignment, but also additional signal components due to vehicle acceleration. Thus, the information from the gyroscope signal should be used for the attitude estimation of a moving vehicle. Taking this into account, the following modification of the algorithm was proposed. The Kalman gain matrix values are set to zero, when the vehicle has velocity change more than certain value during 1 second. This value of velocity (0.15 m/s) change was determined empirically. The state transition matrix $\mathbf{\Phi}$ is replaced by the corresponding identity matrix ($\mathbf{\Phi = I}$), when the vehicle has velocity change less than 0.15 m/s during 1 second [10].

The results of the vehicle attitude estimation are shown in Fig. 4.7-4.9. The vehicle was stationary for the first 60 seconds and the last 10 seconds of the experiment. As expected, the estimation of the pitch and roll based on accelerometer data (when vehicle is stationary) has less fluctuations comparing with the attitude estimation, when the vehicle is moving [10].

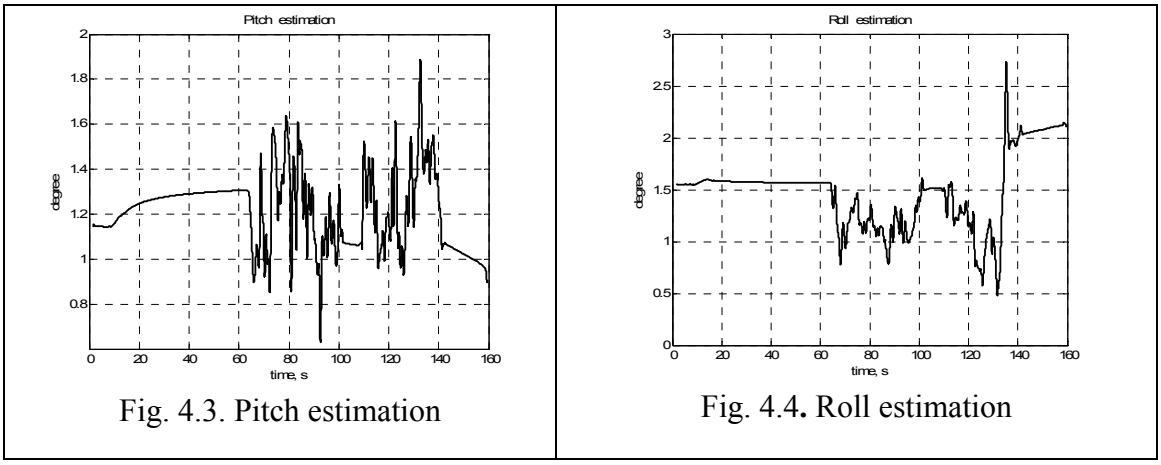

Fig. 4.3. Pitch estimation

Fig. 4.4**.** Roll estimation

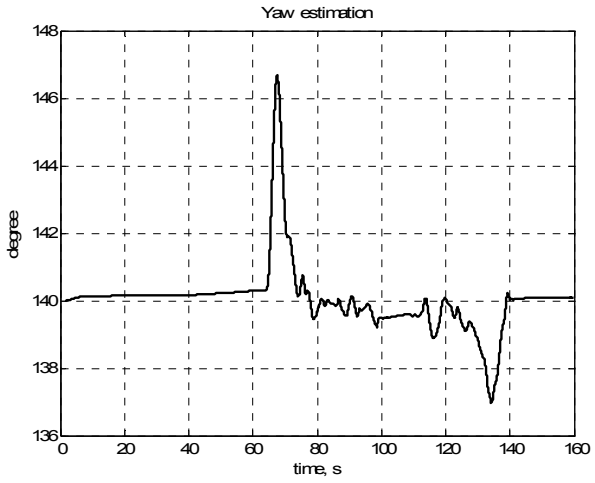

Fig. 4.5. Yaw estimation

5. ESTIMATION ALGORITHMS

Estimation algorithms are used for navigation solution calculating using available data from the sensors. The KF-based algorithms are widely used for this purpose.

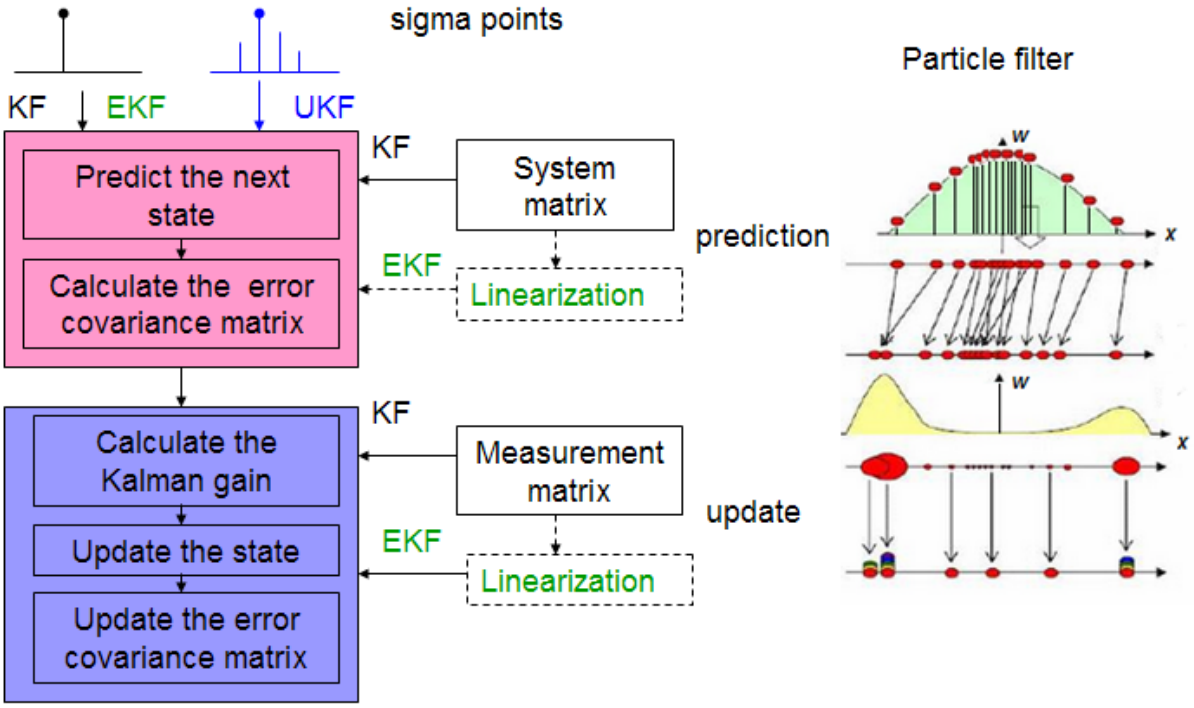

Fig. 5.1. Simplified comparison of LKF, EKF, UKF and PF algorithm.

Usually, the navigation system is modeled as nonlinear dynamic system and appropriate estimation algorithms should be used taking in account nonlinearity of the system. The EKF is considered as a standard estimation algorithm used in modern navigation systems. EKF uses linear approximation (made by Taylor series) of the nonlinear model of the navigation system. The standard KF is used if the considered estimation problem can be described by linear system. The advantage of the LKF is simple implementation and low computational burden.

Simplified comparison of the estimation algorithms (the LKF, EKF, UKF and PF) operating for the system with one state is shown in Fig. 5.1. Algorithms comprise prediction and update step. The UKF algorithm working principle is different from the LKF and EKF, as in the input of the UKF, there are several estimations (sigma points) of one state of the system. Sigma points make approximation of state mean value and covariance. Then these sigma points are processed by the UKF algorithm. The particle filter processes even more state estimations (can be more than 100). These estimations make approximation of the PDF of the system state.

One of the LKF drawbacks is limited estimation capability e.g. no possible to estimate scale factor of the sensors. Thus, it is necessary to develop specific modification of the LKF in order to improve estimation performance. These modifications are considered below (see section 5.1 and 5.3).

5.1. Kalman gain matrix correction algorithm

The designed Kalman gain matrix correction algorithm (KGCA) can be used to decrease system state variables (position, velocity) estimation errors [5]. The algorithm steps are :

a) Step 1: to detect time epoch when acceleration start to change;

b) Step 2: to add special function values to diagonal elements of the Kalman gain matrix in order to improve the algorithm performance during vehicle velocity change and post change period.

Therefore, equations for the Kalman gain matrix updating and correcting are following:

$$\begin{aligned} \mathbf{K}_k &= \mathbf{P}_{k\,(predicted)}\mathbf{H}_k^T(\mathbf{H}_k\mathbf{P}_{k\,(predicted)}\mathbf{H}_k^T+\mathbf{R}_k), \\ \mathbf{F}_k &= diag_{\ell}\{f_{\ell}\}, \\ \mathbf{K}_{k(corrected)} &= \mathbf{K}_k+\mathbf{F}_k, \end{aligned} \tag{5.1}$$

where f - special function's values at time epoch k, ℓ - number of state variables in the dynamic system model.

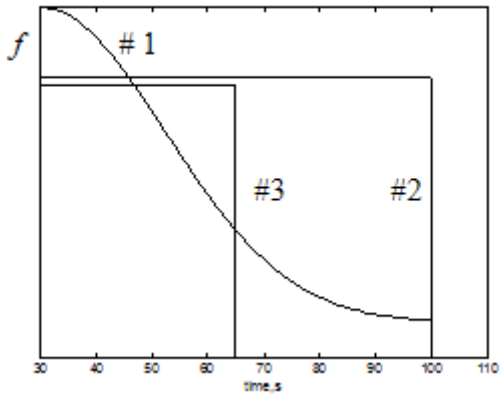

Fig. 5.2. Profiles of three types of the function f

Table 5.1.

Three types of functions

MSE error of position estimation using KGCA and three types of function			
function	#1	#2	#3
MSE	26	300	2569

Three functions, f, were tested. The general forms of these functions are shown in Fig. 5.2. The duration of those functions is defined taking in account duration of the estimation error with high values, i.e. from t = 30 s till t = 100 s (see Fig. 5.2). The MSE error of estimated position (using these functions for correction in (5.1)) when acceleration a_x = 10 m/s^2 take place from t = 30 s till t = 50 s are shown in the Table 5.1 [5].

Simulating results show that function #1, used for the Kalman gain matrix correction, allows reducing estimation error of position in a greater degree. The reason of this can be that the function #1 has smooth transition and, hence the Kalman gain correction is conducted softly without extra disturbance just after the acceleration has changed. The mathematical description of function #1 is [5]

$$f(t_k) = Ae^{-B(t_k - t_D)^2}, \tag{5.2}$$

where A, B - fixed values are decided by user or designer, t_D - time epoch, when acceleration has changed.

5.2. GPS and accelerometer data fusion using LKF

The LKF was applied for the estimation of the distance traveled by land vehicle.

The estimation results of the distance traveled by vehicle with velocities 40, 60, 80 km/h are represented in Table 5.2 [6]. The LKF (total state implementation) was used for GPS and accelerometer data fusion. The precision of the estimated distance is very good for both methods as we can see from Table 5.2. The mean error is 5.33 m for the direct method of the distance estimation that is based only on GPS measurements. The mean error is 4.67 m for the combined GPS and accelerometer data processing method using LKF.

Table 5.2.

Estimation of the distance traveled by vehicle

The distance to be passed by vehicle is 1004±1m	Distance estimation method	
	direct using only GPS data	fusion of GPS and accelerometer data
TEST 1 with v = 40 km/h	1008 m	1007 m
TEST 2 with v = 60 km/h	1009 m	1009 m
TEST 3 with v = 80 km/h	1011 m	1010 m

5.3. Intelligent Kalman filter algorithm

The goal of the calculated distance values processing by an intelligent algorithm - is error decreasing of distance estimation [7]. This error occurs mainly due the noise and uncertainty of the measured values by GPS sensor.

The distance is determined by successive summing up of distances between adjacent points, which coordinates in ECEF frame defined by GPS measurements:

$$s_{x\_GPS,i} = s_{x\_GPS,i-1} + s_{x\_GPS,i,i-1} \tag{5.3}$$

where

$s_{x\_GPS,i}$ –passed distance value at time $t=t_i$;$s_{x\_GPS,i-1}$-passed distance value at time $t=t_{i-1}$;

$s_{x\_GPS,i,i-1}$-passed distance during time period [t_{i-1} t_i] measurement.

The rule of intelligent algorithm applied to passed distance measurements is following [7]:

$$\begin{aligned} s_{x\_GPS,i} &= s_{x\_GPS,i-1} + s_{x\_GPS,i,i-1} \text{ if } a_x > \gamma \text{ at time } t=t_{i-3},\ t_{i-2},\ t_{i-1}, \\ s_{x\_GPS,i} &= s_{x\_GPS,i-1} + 0 \qquad \text{if } a_x \le \gamma \text{ at time } t=t_{i-3},\ t_{i-2},\ t_{i-1}, \end{aligned} \tag{5.4}$$

where a_x- estimated accelerometer signal;γ -defined threshold, that correspond to noisy level of estimated acceleration signal; $s_{x\_GPS,i}$ - driving distance at time $t=t_i$; $s_{x\_GPS,i-1}$-driving distance value at time $t=t_{i-1}$;$s_{x\_GPS,i,i-1}$-driving distance during time period [t_{i-1} t_i].

This rule was defined experimentally through analysis of the accelerometer signals, measured by the sensor during different modes of vehicle movement, and values of driving distance measured by digital measuring wheel DigiRoller Plus II. The main idea of this rule is to exclude distance increasing due to the uncertainty of GPS measurements and uncompensated measurement noise of accelerometer.

Experiments show that the value of γ depends on the vehicle movement mode, type of the road. Having information about driving distance value measured by DigiRoller Plus II, it is possible to find optimal values of γ (when the distance estimation error approaches to minimum); and also relationship between the vehicle movement mode and value of γ [7].

For the case of moderate dynamic mode of vehicle movement (velocities up to 90 km/h) the optimal values of parameter γ are almost the same for these three tests: γ =[0.16… 0.18]. For the case of low dynamic mode of vehicle movement (velocities up to 50 km/h), optimal values of parameter γ are almost the same: γ =[0.04…0.05]. These results are very important as give us quite narrow range of optimal γ to be used in developed algorithm in order to obtain reliable distance estimation for different types of vehicle movement.

The experiments were conducted for different vehicle movement velocities: 40 km/h, 80 km/h and for two types of road: road with asphalt covering and earth road. The reference value of distance was obtained by measuring wheel and the passed distance by vehicle was always the same and equal 1005 m.

Table 5.3.

Distance estimation error for the KF and IKF algorithm

Test #	**Distance estimation error, m**		**Test description (velocity, road)**
	KF	**IKF**	
1	38	9	40 km/h , earth road
2	21	5	50 km/h, asphalt road
3	22	6	40 km/h, asphalt road
4	15	6	80-90 km/h, asphalt road
5	20	5	80-90 km/h, asphalt road
6	21	1	80-90 km/h, asphalt road

It is evident from Table 5.3 that the IKF algorithm has better estimation (more precise) of the passed distance [7].

5.4. 1-D navigation system with EKF estimation algorithm

The implementation scheme of such navigation system with EKF is shown in Fig. 5.3.

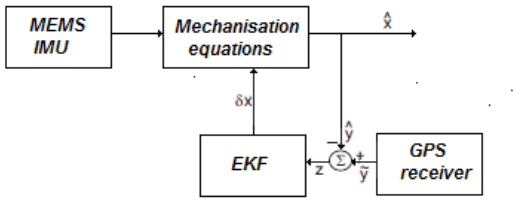

Fig. 5.3. Closed loop implementation of EKF

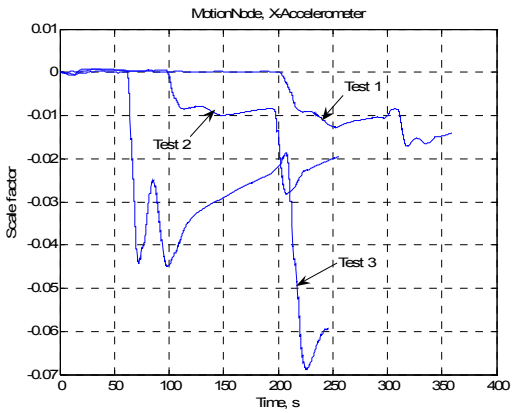

Fig. 5.4. Estimates of scale factor of MEMS accelerometer

Here, the errors estimated by the EKF are fed back every iteration, to correct the system itself, zeroing Kalman filter states in process. This feedback process keeps the Kalman filter states small, minimizing the effect of neglecting high order products of the states in the system model [17].

Accelerometer scale factor is not possible to estimate using the LKF. Thus, the EKF is used for sensor scale factor estimation. The sensors data was obtained during field tests. The estimated scale factors of the accelerometer according data from three experiments are shown in Fig. 5.4 [9].

The step jumps of the estimation of scale factor are due to the switch over from the stage when system state (scale factor) is not observable due to the almost zero value of vehicle acceleration to the stage with observable state, when the acceleration is not zero. The worst estimation is found for test #3. The reason of this is less exact synchronization of GPS and IMU data achieved for this test.

5.5. Unscented Kalman Filter

The main disadvantage of the PF is high computational resource requirement and poor algorithm stability characteristics. When using the EKF algorithm, it requires appropriate linearization of nonlinear problem and the performance become poor, when the error states become large. The UKF filter can be considered as compromised choice between the PF and EKF. Of course, if the estimated system can be described by linear model, the LKF is preferable choice. Thus, the UKF estimation algorithm was selected for use in MEMS based integrated navigation system, which integrates results of investigation of this work.

The block diagram of such system is shown in Fig. 5.5. Equipment installation inside car is shown in Fig. 5.6

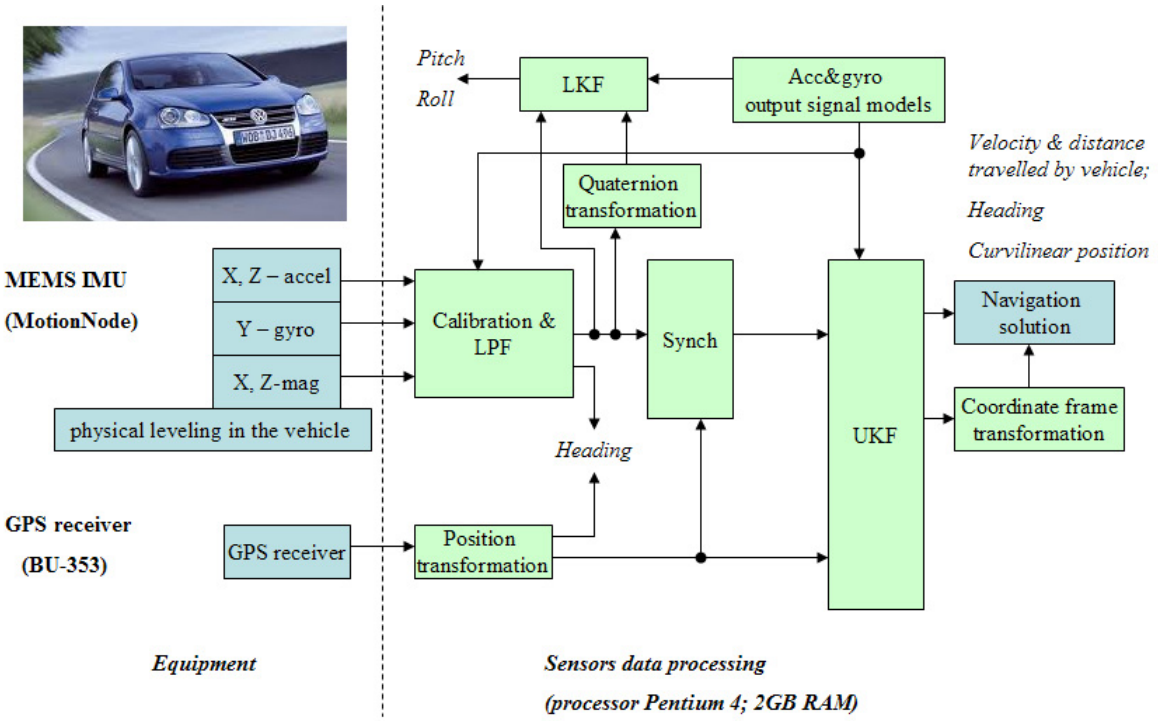

Fig. 5.5. Implementation of the GPS/MEMS IMU integrated navigation system

The fusion algorithm (UKF) of sensor data consists of the prediction and updating step. For the prediction step, the frequency f_2 = 50 Hz was chosen. This frequency perfectly suits for our experiments, since the land vehicle is not moving faster than 30 m/s. The frequency of the updating step is equal to the GPS output data rate f_1 = 1 Hz. This GPS data is used to compensate measurement errors in the accelerometers and gyroscope readings [11].

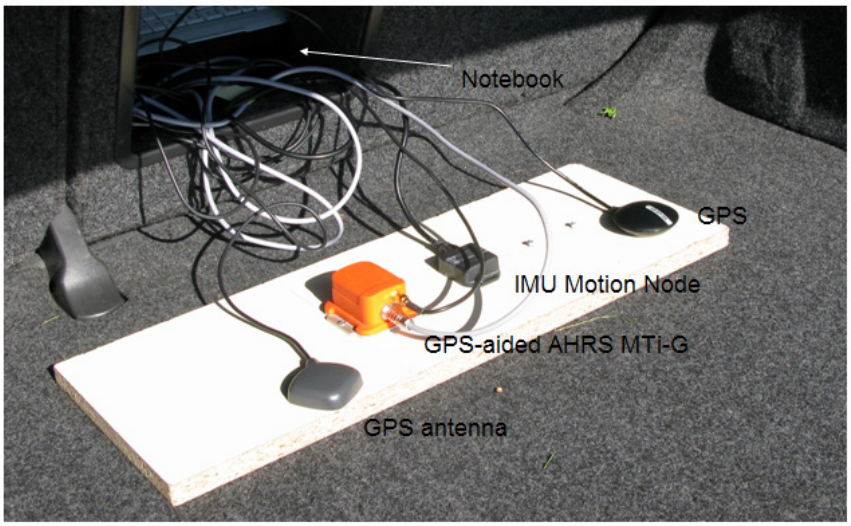

Fig. 5.6. Equipment installation inside land vehicle

The navigation system state vector selected for the UKF is:

$$\mathbf{x}_k = [b_{a_x} \quad b_{a_z} \quad a_x \quad a_z \quad v_x \quad v_z \quad b_{w_y} \quad w_y \quad \phi], \tag{5.9}$$

where b_{a_x} and b_{a_z} are the estimates of accelerometer biases, a_x and a_z are the estimates of acceleration along x-axis and z-axis, v_x and v_z are the estimates of velocities along x-axis and z-axis of the vehicle coordinate frame, b_{g_y} is the estimate of gyroscope signal bias , w_y is the estimate of angular rate of vehicle around y-axis of vehicle coordinate frame, ϕ is the estimate of the heading of the vehicle. The orientation of the vehicle coordinate frame is shown in the Fig. 5.7. The longitudinal axis of the vehicle coordinate system is *x*. The lateral axis of the vehicle coordinate system is *z*, and the y-axis points downwards. The IMU is placed in the car in order the IMU x-axis and z-axis has the same orientation with the vehicle longitudinal and lateral axis.

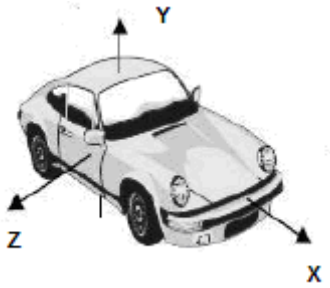

Fig. 5.7. The vehicle coordinate frame

The navigation system state vector is propagated with the frequency f_2 = 50 Hz between measurements using the following equations [11]:

$$\hat{b}^-_{a_x,i+1} = \beta_1 \cdot \hat{b}^-_{a_x,i}, \tag{5.10}$$

$$\hat{b}^-_{a_z,i+1} = \beta_2 \cdot \hat{b}^-_{a_z,i}, \tag{5.11}$$

$$\hat{b}^-_{w_y,i+1} = \beta_3 \cdot \hat{b}^-_{w_y,i}, \tag{5.12}$$

$$\hat{a}^-_{x,i+1} = 0.5 \cdot (f_{x,i} + f_{x,i-1}) + \hat{b}^-_{a_x,i}, \tag{5.13}$$

$$\hat{a}^-_{z,i+1} = 0.5 \cdot (f_{z,i} + f_{z,i-1}) + \hat{b}^-_{a_z,i}, \tag{5.14}$$

$$\hat{w}^-_{y,i+1} = 0.5 \cdot (\varphi_{y,i} + \varphi_{y,i-1}) + \hat{b}^-_{w_y,i}, \tag{5.15}$$

$$\hat{v}^-_{x,i+1} = \hat{v}^-_{x,i} + T \cdot \hat{a}^-_{x,i+1}, \tag{5.16}$$

$$\hat{v}^-_{z,i+1} = \hat{v}^-_{z,i} + T \cdot \hat{a}^-_{z,i+1}, \tag{5.17}$$

$$\hat{\phi}^-_{y,i+1} = \hat{\phi}^-_{y,i} + T \cdot \hat{w}^-_{y,i+1}, \tag{5.18}$$

where β_1, β_2, β_3 are the fading factors; $f_{x,i}$, $f_{z,i}$ are the raw measurements of MEMS accelerometers, $\varphi_{y,i}$ is the raw measurement of MEMS gyroscope, T is the sampling time. The values for the fading factors were determined experimentally during the process of adjusting algorithm parameters in order to guarantee acceptable performance of the algorithm, i.e. minimal estimation error of the vehicle velocity. In most of the cases the fading factors were equal to 0.9999.

The navigation system measurement vector is [11]:

$$y_k = [v_N \quad v_E], \tag{5.19}$$

where v_E is the east component of the vehicle velocity, v_N - is the north component of the vehicle velocity.

The observation model is given by the following nonlinear equations [11]:

$$\hat{v}_{N,k} = \sqrt{[(\hat{v}_{x,k}^{-})^2 + (\hat{v}_{z,k}^{-})^2]} \cdot \cos(\hat{\phi}_{y,k}^{-}), \tag{5.20}$$

$$\hat{v}_{E,k} = \sqrt{[(\hat{v}_{x,k}^{-})^2 + (\hat{v}_{z,k}^{-})^2]} \cdot \sin(\hat{\phi}_{y,k}^{-}). \tag{5.21}$$

These nonlinear equations are directly used in the UKF algorithm.

Fig. 5.8. Trajectory estimation of the moving land vehicle (blue curve). TEST Jan2

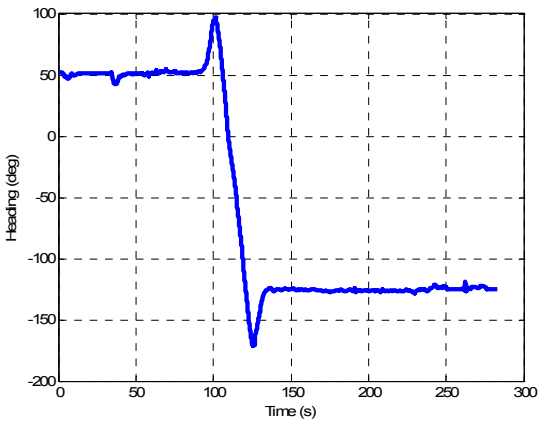

Fig. 5.9. The heading estimation. TEST Jan2

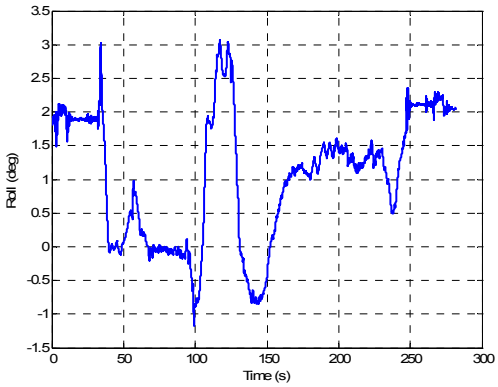

Fig. 5.10. The roll estimation. TEST Jan2

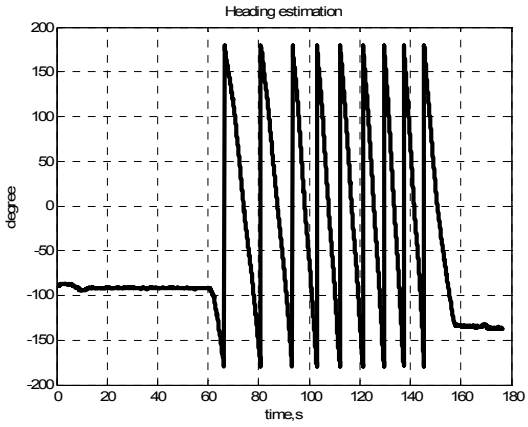

Fig. 5.11. The heading estimation. TEST Jan9

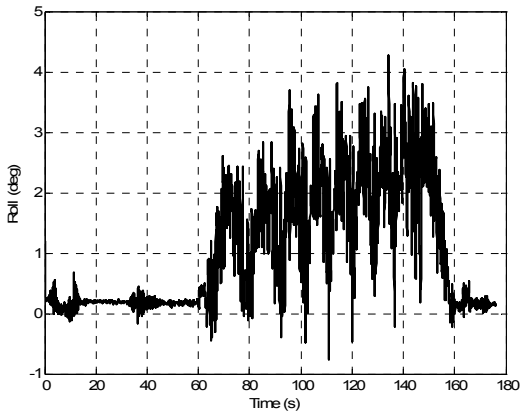

Fig. 5.12. The roll estimation. TEST Jan9

The field experiment were conducted for the kinematics data collection of moving land vehicle and then position was estimated using described above algorithm. The estimated trajectory in the navigation coordinate frame (ENU) was superimposed on the map provided by (c) 2013 Google. The results of moving vehicle trajectory estimation are shown in the Fig. 5.8.

The results of the vehicle attitude estimation are shown in Fig. 5.9-5.12. These results are obtained using magnetometers data processing and LKF (for accelerometer and gyroscope data fusion).

6. ESTIMATION ALGORITHMS PERFORMANCE DURING GPS OUTAGE

Here the performance results of the navigation solution during GPS signal outages are presented. The sensor data was obtained during field kinematics tests. The car was driven on the asphalt road during field tests. The vehicle movement trajectory is shown in the Fig. 6.1.

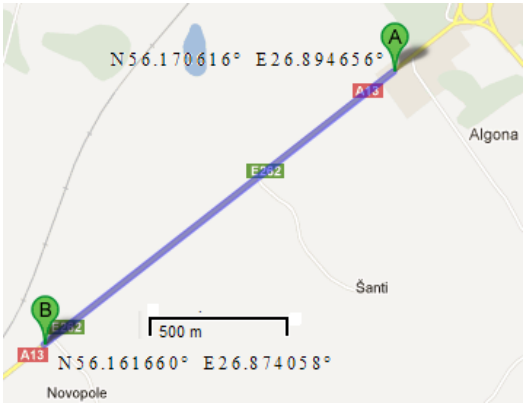

Fig. 6.1. Vehicle movement trajectory on the map [9]

6.1. Adaptive EKF

The GPS signal outages rise more serious problem of proper KF-based algorithm adjusting and navigation system performance increasing. Innovation based adaptive estimation techniques for the EKF can be used in order to fix such problem The vehicle velocity estimation (Test1) during simulating GPS outages is shown in Fig. 6.2 [9].

The velocity error increases with time, when standard EKF used, whereas the velocity estimation by the adaptive EKF is very near to reference value. The reference velocity corresponds to estimated velocity, when the GPS measurements are available.

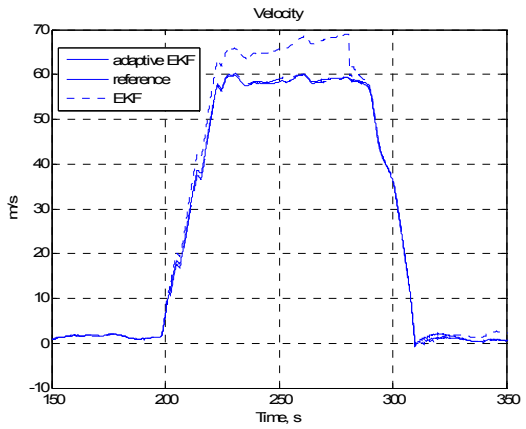

Fig. 6.2. Vehicle velocity estimation during 80 s of GPS signal outage at time from 200 s till 280 s

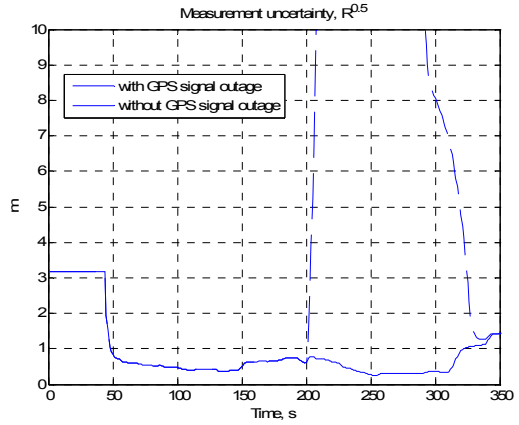

Fig. 6.3. Estimation of **R** value by adaptive EKF

The adaptation process of position measurement noise value for Test 1 is shown in Fig. 6.3. During period of GPS signal outage, we see abrupt increase of **R** value, because uncertainty of position measurements increase, as GPS signal is blocked.

The results of compare for conventional and adaptive EKF during GPS signal outage simulating are presented in Table 6.1. The position and velocity estimation error are much smaller for adaptive EKF except Test 3, where difference is not so big. The reason of this is that parameters of the conventional EKF for Test 3 were carefully adjusted by numerous data processing cycles and even with this huge effort, the performance didn't reach one of the adaptive EKF [9].

Table 6.1.

EKF algorithm performance analyze during GPS signal outage

Test #	**Velocity***	**Period of GPS signal outage**	**RMSE** of velocity, EKF**	**RMSE** of velocity, adaptive EKF**
1	60km/h	200…280 s	6.70 km/h	0.54 km/h
2	60km/h	80…160 s	6.11 km/h	1.74 km/h
3	70km/h	60…160 s	4.79 km/h	1.72 km/h

* typical profile of velocity during test is shown in Fig. 8.2
** RMSE value during period of GPS signal outage

Again not perfect results of Test 3 for position estimation with the adaptive EKF can be explained by imperfection of the GPS and IMU data synchronization [9].

6.2. UKF algorithm

The analysed velocity profile in the following tests contains different types of the vehicle motion: stationary periods during $t \in \{0...82\}s$ and $t \in \{175...198\}s$, high dynamic periods with variable acceleration of the vehicle during $t \in \{82...115\}s$ and $t \in \{137...175\}s$, period with nearly constant vehicle velocity $t \in \{115...137\}s$ [11]. The GPS signal outages are simulated during mentioned above time periods of the vehicle moving for the comparative performance analysis of the sensor data processing algorithms. The tuning parameters of data processing algorithms remain identical for each of the analysed GPS signal outage simulation case.

The KF, EKF and UKF performance analysis for stationary mode is given in Table 6.2. The GPS signal outage time was equal to 60 s for each simulation. Only the starting time for GPS signal outage was different, so that the time period, when the vehicle was in the stationary mode with the presence of the GPS signal, with each next simulation was increased by 5 s. The velocity estimation error (RMSE) continuously decreases (for the EKF and the UKF) with increasing of the initial time of the vehicle stationary mode with the presence of GPS signal. This is correct behavior of the algorithm, which correctly estimates errors of the inertial sensors and adequately models considered here low-cost integrated navigation system. As we can see from Table 6.2, the velocity estimation error was smaller for the UKF algorithm except the cases when the initial time (in this case it is 5-6 s) for the UKF algorithm adaptation was not enough [11].

The velocity estimation errors for high dynamic mode of the vehicle motion are presented in Table 6.3. Very good performance metrics for the KF, when vehicle was moving with nearly constant velocity, are not surprising, because parameters (acceleration and velocity of the vehicle, accelerometer bias) of the system changes slowly during small GPS signal outage period and hence it can be easily predicted by KF. In all other cases the UKF algorithm considerably outperforms the KF and the EKF algorithms. The rather high value of the velocity estimation error (RMSE) by the UKF for GPS signal outage during 120…180 s can be explained by the fact that the GPS outage period starts quite quickly after high dynamic mode of the car motion. This does not allow for the UKF to stabilize state estimates [11].

Table 6.2.

Velocity estimation errors* during GPS signal outage

Period of GPS outage	**KF**		**EKF**		**UKF**	
	RMSE km/h	**ΔV, km/h**	**RMSE km/h**	**ΔV, km/h**	**RMSE km/h**	**ΔV, km/h**
5…65 s	20.7	36.0	19.0	33.0	24.3	41.0
6…66 s	9.2	16.0	17.6	31.0	22.0	37.0
10…70 s	6.6	11.0	15.2	26.0	13.1	22.0
15…75 s	13.9	26.0	9.0	18.0	8.0	13.5
20…80 s	6.7	13.5	6.8	13.0	3.5	5.7
21…81 s	15.8	27.0	5.4	10.7	3.3	5.4

* estimation errors include RMSE of velocity estimate (RMSE) and absolute maximal estimated velocity error (ΔV**)** during GPS signal outage.

Table 6.3.

Velocity estimation errors* during GPS signal outage

Period of GPS outage	KF		EKF		UKF	
	RMSE, km/h	ΔV, km/h	RMSE, km/h	ΔV, km/h	RMSE, km/h	ΔV, km/h
20…120 s	40.8	95.0	20.2	41.0	3.3	5.7
120..180 s	33.3	74.0	18.2	33.0	7.3	11.0
20…180 s	60.1	103.0	23.6	41.0	8.1	20.0
116..136 s	3.24	7.0	5.9	10.0	5.4	7.0
120..130 s	3.1	5.0	1.7	2.8	2.1	2.5

* estimation errors include RMSE of velocity estimate (RMSE) and absolute maximal estimated velocity error (ΔV) during GPS signal outage.

The velocity estimation error (for the KF, EKF, UKF) reaches maximum (ΔV) in the end of GPS signal outage period, when the car was in stationary mode or moving with nearly constant velocity, but that's not necessarily the case, when the car was moving with variable acceleration.

The comparative performance analysis of the UKF, EKF and KF for the car velocity estimation was performed for different dynamic mode of the vehicle movement during GPS signal outages.

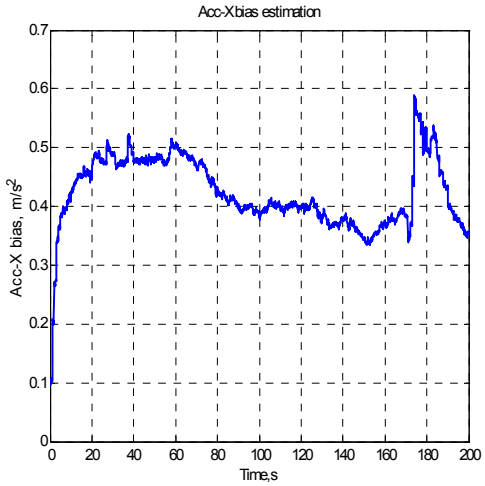

Fig.6.4. Estimate of the accelerometer bias velocity

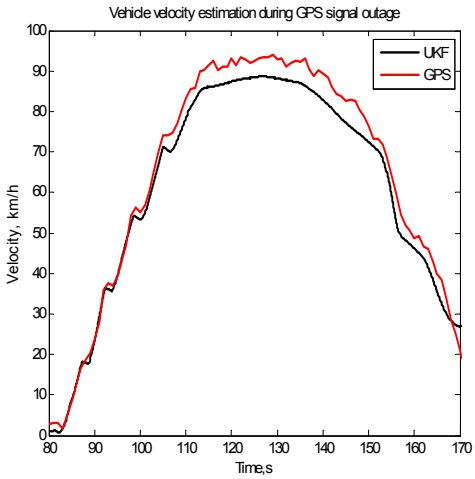

Fig.6.5. Estimate of the vehicle

The UKF algorithm, adapted for the low-cost sensors data processing, has smaller velocity estimation error during GPS signal outages comparing with the EKF algorithm. This is especially obvious for the cases, when vehicle has experienced quick changes in the car dynamics.

The estimate of the vehicle velocity (using UKF) during GPS signal outage period is shown in Fig. 6.5. The estimate of x-accelerometer bias is shown in Fig. 6.4. The reference velocity is estimated using GPS data (see Fig.6.5).

CONCLUSIONS

In the process of performing the tasks required to meet the goals of the research stated in the introduction chapter, the following main results were obtained:

1. The experimental analysis of the noise characteristics of the MotionNode IMU inertial sensors produced following results:
   a) the useful signal frequency bandwidth was estimated for inertial sensors;
   b) the noise types of the accelerometers and gyroscopes signals were identified;
   b) the MotionNode IMU requires a warming up period of 10-20 min for more reliable and precise navigation solution calculation;
   c) the magnetometers require recalibration whenever its surrounding environment is changed, for example, when the unit location is moved within the car;
   d) the Gaussian PDF is suitable approximation of probability distribution function of the MotionNode accelerometer measurement error for short periods (several minutes);
   e) the spectrogram and data frame statistical analysis (including AV) of MEMS sensors signals provide essential information about its characteristics.

2. The signal models of the MotionNode IMU sensors were developed:
   a) the in-run bias of lateral and longitudinal accelerometer and vertical channel gyroscope of MotionNode IMU can be modelled using sum of deterministic function and stochastic function;
   b) constant part of the run-to-run bias of the stationary accelerometer can be estimated as mode value of it error signal using less than 100 samples of the data.

3. The performed analysis of the sensor data processing algorithms showed:
   a) MEMS accelerometers can be used for the pitch and roll estimation in the static mode with sufficient precision, when denoising algorithms are additionally used (the precision (1σ) of the roll/pitch estimation is equal to 0.03 deg);
   b) the heading estimation using GPS and magnetometer data has similar results for in-motion land vehicle (the precision (1σ) of the heading estimation is equal to 0.3 deg in motion);
   c) for attitude estimation in both the static and in-motion position, adaptive algorithm for accelerometer, and gyroscope data processing with detection of driving mode is required.
   4. The modifications (KGCA and IKF) of the LKF improves accuracy (the achieved result is 30%) of the driving distance estimation.

5. The most suitable signal denoising algorithms (Chebyshev type II filter, wavelet transform and LKF) and its combinations were experimentally investigated for selecting the most appropriate method for reducing of the high frequency measurement noise of MEMS sensors. The combination Chebyshev type II filter +LKF shows the best results.

6. The following findings allow simplifying implementation of the sensor data processing algorithms:
6.1. It was proved that contributions of the Earth and transport rate component are minor comparing the measurement noises of MotionNode inertial sensors. Especially this is true for MEMS gyroscope; hence, it is possible to neglect this contribution for MEMS gyroscope;
6.2. It was proved that contribution of the Earth and transport rate component can be included and modeled in the static part of the accelerometer bias, when the land vehicle heading is not

changing. When the vehicle heading is changing, then this contribution is changing too. The range of changing is ~10^{-3} m/s^2. This can be modeled using deterministic function;
6.3. It was shown that in order to simplify navigation algorithm without introducing additional errors in navigation solution, the IMU coordinate frame (b-frame) should be aligned with the v-frame and n-frame.

7. The particle filter and the Kalman-based estimation algorithms (the LKF, EKF, and UKF) were investigated and adjusted for use in navigation processor and tested using experimental test data. The UKF algorithm was defined as preferable option for use in navigation processor, because of the convenient and straightforward method of the system and measurement model definition, tuning capability and estimation precision during GPS signal outages with period t = 60 ...90 s. The particle filter requires high computational burden that may not be acceptable for the low-cost navigation systems. The operating stability of the simplest PF was not acceptable. The EKF requires linearization of the nonlinear dynamic system. This can be often nontrivial problem for MEMS-based navigation system, even without solution. The major drawback of the KF-based algorithms implementation in GPS/MEMS IMU integrated navigation system is considerable time and efforts needed for algorithm tuning.

8. The performance of the developed GPS/MEMS IMU integrated navigation system was evaluated using field test data that includes simulated periods of the GPS signal outages. The UKF algorithm has smaller velocity estimation error during GPS signal outages comparing with the LKF, EKF algorithm. This is especially obvious for the cases, when vehicle has experienced quick changes in the dynamics of the car movement.

9. The architecture of the GPS/MEMS IMU integrated navigation system (including navigation processor) and the design methodology of MEMS-based integrated navigation system with specified performance and reduced computational burden were developed.

10. It was shown that GPS/MEMS accelerometer integrated system can provide additional information about car (door opening and closing, engine switching on/off, passenger moving inside car) with exact timing of the event.

FUTURE WORK

1. To elaborate the self-tuning inertial data processing systems with optimal performance (basing on the LKF and the UKF) according vehicle movement dynamics.
2. To elaborate the adaptive models of the output signal for low-quality inertial sensors.
3. To increase an autonomous operating time of the low-quality inertial sensors with achieving specified performance characteristics for the land vehicle navigation.
4. To elaborate MEMS gyroscopes data processing algorithms for increasing precision of attitude estimation.
5. To investigate the GPS measurement accuracy impact on low-cost integrated land vehicle navigation system.

BIBLIOGRAPHY

1. Acar Cenk, Shkel Andrei. MEMS vibaratory gyroscopes.- Springer Science, 2009, -262 p.
2. Aggarwal Priyanka, Syed Zainab Noureldin Aboelmagd and El-Sheimy Naser, MEMS-Based Integrated Navigation. London: Artech House, 2010.
3. Bekir Esmat. Introduction to Modern Navigation Systems. – Singapore:World Scientific Publishing Co, 2007.-255 p.
4. Bistrovs V. Analyze of MEMS Based Inertial sensors Parameters for land Vehicle Navigation Application// *RTU zinātniskie* raksti. 7. sēr., Telekomunikācijas un elektronika. – Riga: RTU, 2008. - Vol. 8. - pp. 43-47.
5. Bistrovs V. Analyse of Kalman Algorithm for Different Movement Modes of Land Mobile Object // Electronics and Electrical Engineering, ISSN 1392-1215. - 2008 Nr.6 (86).- pp. 89.-92
6. Bistrovs V., Kluga A. Combined Information Processing from GPS and IMU using Kalman Filtering Algorithm // Electronics and Electrical Engineering, ISSN 1392-1215. - 2009, No. 5(93).- pp. 15-20
7. Bistrovs V., Kluga A. Distance Estimation using Intelligent Fusion of Navigation Data// Electronics and Electrical Engineering, ISSN 1392-1215. - 2010, No. 5(101).- pp. 47-52.
8. Bistrov V. Study of the characteristics of Random Errors in Measurements by MEMS Inertial Sensors// Automatic Control and Computer Sciences. - Allerton Press 2011, Vol. 45, No. 5, pp. 284–292.
9. Bistrovs V., Kluga A. Adaptive Extended Kalman Filter for Aided Inertial Navigation System// Electronics and Electrical Engineering, – Kaunas:Technologija 2012. – No. 6(122). – pp. 37–40.
10. Bistrov V. Performance analysis of alignment process of MEMS IMU // International Journal of Navigation and Observation, Volume 2012, 2012/
11. Bistrovs V., Kluga A. The Analysis of UKF based Navigation during GPS outage// Electronics and Electrical *Engineering*, – Kaunas:Technologija 2013 Vol 19, No 10. – P.13 – 16
12. Brown R. G., Hwang Y. C.. Introduction to random signals and applied Kalman filtering. - New York: J. Wiley, 4d edition, 2012. – 400 p.
13. El-Rabbany Ahmed. Introduction to GPS. The Global Positioning System. - Boston London: Artech House, 2002, 176 p.
14. Farrell Jay A. Aided Navigation. – New York: McGraw-Hill, 2008.
15. Godha S., Cannon M. E. GPS/MEMS INS integrated system for navigation in urban areas// GPS Solut , 2007, No. 11, p.193–203
16. Grewal M., Weill L., Andrews A. Global Positioning Systems, Inertial Navigation, and Integration .- New Jersey: John Wiley & Sons, Inc., 2007. -525 p.
17. Groves Paul D., Principles of GNSS, Inertial, and Multisensor Integrated Navigation Systems. Second Edition London: Artech House, 2013.-776 p.
18. Gustafsson F., "Particle filter theory and practice withpositioning applications//"Aerospace and ElectronicSystems Magazine, IEEE, 2010,vol. 25, no. 7.- pp. 53–82.
19. Honglei Qin, Li Cong, Xingli Sun. Accuracy improvement of GPS/MEMS-INS integrated navigation system during GPS signal outage for land vehicle navigation// Journal of Systems Engineering and Electronics, 2012, Volume 23, Issue 2.- pp. 256-264
20. Kaplan Elliott D., Christopher J. Hegarty Understanding GPS: Principles and Applications. - Artech House, 2005 - 723 p.

21. Kealy Allison , Retscher Günther, Grejner-Brzezinska Dorota, Vassilis. Gikas , Gethin Roberts.- Evaluating the performance of MEMS based inertial navigation sensors for land mobile applications//Archives of Photogrammetry, Cartography and Remote Sensing, Vol. 22, 2011.- pp. 237-248.
22. Mohd-Yasin F., Nagel D. J. and Korman C. E. Noise in MEMS Measurement science and technology 21, 2010.-pp. 1-22 .
23. Nassar S., Schwarz, K.P., El-Sheimy N. INS and INS/GPS Accuracy Improvement Using Autoregressive (AR) Modeling of INS Sensor Errors// Proceedings of the ION 2004 National Technical Meeting (NTM 2004), San Diego, California, USA, January 26-28, 2004.
24. Noureldin Aboelmagd, Tashfeen B. Karamat, Jacques Georgy. Fundamentals of Inertial Navigation, Satellite-based Positioning and their Integration.-Springer, 2013.- 313 p.
25. Otman Ali Awin, Application of Extended kalman filter algorithm in SDINS/GPS Integrated Inertial navigation system// Applied Mechanics and Materials, 2013, p. 528-535
26. Salychev Oleg S. MEMS-based Inertial Navigation:Expectations and Reality.- BMSTU Press, Moscow, Russia, 2012.-208 p.
27. Soken, H. and Hajiyev, C. (2013). Adaptive Fading UKF with Q-Adaptation: Application to Picosatellite Attitude Estimation. //*J. Aerosp. Eng.*, 26(3), pp. 628–636.
28. Titterton D. et al., Strapdown inertial navigation technology, 2nd edition.- USA: The institution of electrical engineers, 2004. - 558 p.
29. Корнилов А.В. Система ориентации летательного аппарата на интегральных датчиках, Микромеханические системы, Труды Нижегородского государственного технического университета им. Р.Е. Алексеева № 4(83), 2010, стр. 327-332.
30. Federal Agencies Unanimously Say That LightSquared Interferes With GPS System/ Internet.- http: //www.fieldtechnologies.com/federal-agencies-unanimously-say-that-lightsquared-interferes-with-gps-system/